

LETTERS

Competition between Water and Hydrogen Peroxide at Ti Center in Titanium Zeolites. An *ab Initio* Study

Ettore Fois,* Aldo Gamba, and Eleonora Spanó†

DSCA, Università degli Studi dell'Insubria, Via Lucini 3, I-22100 Como, Italy

Received: April 23, 2004; In Final Form: May 22, 2004

A combined Car–Parrinello molecular dynamics blue moon sampling approach has been adopted to study the competitive attack of H₂O and H₂O₂ at a tetracoordinated Titanium site in a Ti–zeolite. The results indicate that, although the attack of water to form a trigonal bipyramidal center is thermodynamically more stable, the attack of hydrogen peroxide to form a similar adduct is kinetically favored. In both cases, solvent cooperation is effective in the formation of the adducts. The relevance of such a result in relation to the catalytic properties of Ti–zeolites is discussed.

Introduction

Titanium silicalite,¹ TS1, is a well-known highly selective catalyst for many oxidation reactions. TS1, a silica-rich zeolite with MFI structure, has been the subject of many investigations^{2–23} aimed at the understanding of the role played by the Ti centers.

Actually, TS1 has been a challenge for both theoreticians and experimentalists competing in the search for the structure of the Ti center in the zeolitic framework and for the mechanism of the oxidative reactions. The catalytic properties of TS1, and other Ti–zeolites as well, are of particular relevance because of the low environmental impact. Indeed, TS1 is able to convert quantitatively, and in mild conditions, light olefins (e.g., propene) into the corresponding epoxides by using a mixture of H₂O/H₂O₂ as oxygen source with the release of water as byproduct.^{2,3}

At low Ti content (TiO₂ less than 3 wt %), Ti isomorphously replaces Si in the zeolitic framework assuming a tetracoordination with four framework oxygen atoms;⁴ however, many structural details related to the mechanism of catalytic cycle

are yet unknown, even if a number of models have been proposed.^{2,18–23}

When dry TS1 interacts with a H₂O/H₂O₂ mixture without organic substrate a yellow labile compound is formed²⁴ (absorbing light at 26 000 cm⁻¹).

The yellow compound is destroyed or disappears unless further H₂O₂ is poured into the system.² The change of color of the sample under contact with the solution of hydrogen peroxide indicates that H₂O₂ chemically reacts with TS1, probably forming an unstable oxidized zeolite.

Zecchina and co-workers²⁴ have recently proposed a possible peroxo structure that could be related to the labile yellow compound. It is believed that such a labile intermediate plays a role in the catalytic cycle. However, the formation mechanism and the structural details of such an unstable complex are yet unknown.

At the microscopic level, the interaction between pure solvent and Ti–zeolite is much more clear. Several studies have been reported^{6–17} on the interactions of dry TS1 with solvent molecules, like H₂O or NH₃, for instance.

A wealth of experiments, based on XANES, EXAFS, infrared, Raman, and UV spectroscopies among others, converged to a picture where the tetrahedral symmetry at the Ti center is disrupted upon absorption of solvent. The tetrahedral TiO₄ acts

* Corresponding author. E-mail: fois@fis.unico.it. Fax: ++39 31 326230.

† Present address: Dipartimento di Scienza dei Materiali, Università di Milano Bicocca, Via Roberto Cozzi 53 I-20125 Milano. Italy.

as a Lewis acid forming penta- or hexacoordinated $\text{Ti}(\text{L})_n\text{O}_4$ centers, where L stands for a generic ligand (solvent) molecule and $n = 1, 2$. In dry Ti–zeolites Ti–O bond distances are about 1.81 Å, whereas Ti–O distances are about 1.84 Å in the presence of solvent and the Ti–L distance is about 2.2 Å.¹⁴ Moreover, a series of ab initio calculations on the Ti center in fully periodic zeolitic (chabasite) systems,^{25,26} indicate that the stability (binding energy) of the $\text{Ti}(\text{L})_n\text{O}_4$ centers with $n = 1$ increases with the basicity of L. For instance, the binding energy for the complex with $\text{L} = \text{NH}_3$ is higher than the one with $\text{L} = \text{H}_2\text{O}$. Recently,²⁷ the relevance of cooperation among solvent molecules in the formation of the TiLO_4 complex in zeolites, for the case $\text{L} = \text{H}_2\text{O}$, has been highlighted.

If one makes the quite reasonable hypothesis that in the formation of the yellow labile complex (H_2O_2 chemisorption) the first step is similar to the adsorption of a L solvent molecule, there could be some difficulty in justifying the overall process. Indeed, as H_2O_2 is a base much weaker than water and because in the $\text{H}_2\text{O}/\text{H}_2\text{O}_2$ mixture the water content is usually 70%, it may be not easy to accept that such a weaker base could replace a ligand, that is, a stronger base and in excess, in an acid–base TiLO_4 complex.

Model and Calculations

Here we present results of ab initio simulations of a Ti–zeolite (offretite) in the presence of both H_2O and H_2O_2 molecules. The aim of this investigation is the study of the energetic and of the activation energies for the formation of a $\text{Ti}(\text{L})\text{O}_4$ center, where the ligand L is water or hydrogen peroxide.

The blue moon ensemble approach²⁸ in the frame of the first principles molecular dynamics scheme²⁹ is adopted in this investigation. Such an approach allows us to study the free energy profile for a process, and typically it has been used in the simulation of chemical reactions;^{30–32} also, recently, the adsorption process of water on different surface sites of TiO_2 has been modeled with this approach.³³ In the case presented here, the adsorption of a molecule L (H_2O or H_2O_2) at the Ti center in the zeolite offretite is studied by ab initio blue moon sampling.

The stoichiometry of the system is $[\text{TiSi}_{17}\text{O}_{36}](\text{H}_2\text{O})(\text{H}_2\text{O}_2)$ with periodic boundary conditions. The chosen framework structure is that of offretite³⁴ (OFF). Ti–OFF has been synthesized, and its catalytic activity in the oxidative reaction of olefins in the presence of a ($\text{H}_2\text{O}/\text{H}_2\text{O}_2$) mixture as the oxygen source has been demonstrated.³⁵ Cell parameters of the hexagonal OFF structure are $a = 13.229$ Å and $b = 7.338$ Å, as adopted in ref 27 for Ti–OFF and in ref 36 for Al–OFF. Such a choice is based on the fact that the cell parameters of Ti–OFF and Al–OFF are found equal in X-ray powder diffraction experiments when the content of Al and Ti are the same in the zeolite.³⁵ A gradient-corrected density functional approximation^{37,38} is adopted for the electronic structure calculations, norm-conserving nonlocal pseudopotentials^{39,40} approximate the core-valence interactions. Kohn–Sham orbitals⁴¹ were expanded in plane waves up to a kinetic energy cutoff of 60 Ry (240 Ry for the density representation). The equations of motion were generated by the Car–Parrinello–Lagrangian²⁹ and numerically integrated⁴² by adopting a time step of 0.121 fs and a fictitious inertia parameter for the coefficients corresponding to 500 au. Nose–Hoover chains of thermostats were used for temperature control.⁴³

After equilibration of such a system at 298 K, two configurations were chosen as starting points for the blue moon samplings,

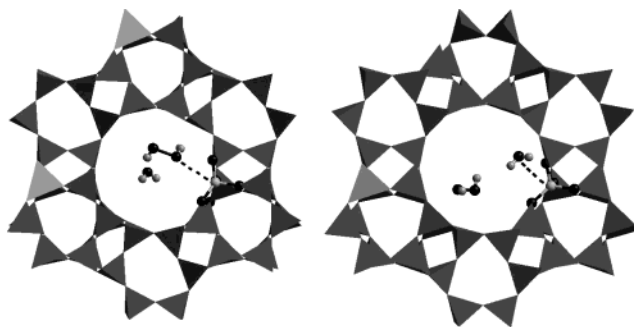


Figure 1. Schematic structural models of the Ti–OFF system. In the left panel, the starting configuration of the blue moon sampling for the insertion of H_2O_2 at a Ti center is represented. In the right panel the same configuration for H_2O insertion. Only the TiO_4 tetrahedron is represented by ball-and-stick; the other SiO_4 tetrahedra are sketched as polyhedra. H_2O and H_2O_2 are represented by ball-and-stick: oxygen as black spheres, hydrogen as gray spheres. Dashed lines represent the constrained distance Q (see text).

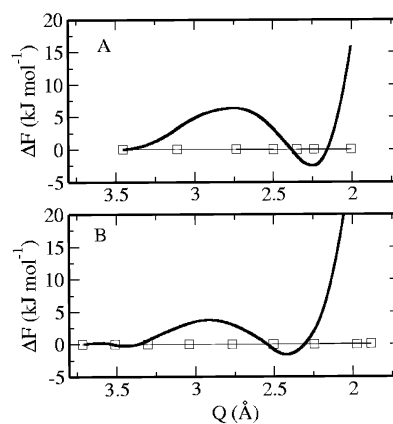


Figure 2. Calculated free energy paths vs Q for the insertion of a ligand L at a Ti center in Ti–OFF. Panel A refers to $\text{L} = \text{H}_2\text{O}$; panel B refers to $\text{L} = \text{H}_2\text{O}_2$. Squares represent the sampled values of Q . Distances in Å, energies in kJ mol^{-1} .

one with H_2O_2 approximately at the center of the large 12-member ring close to the Ti site, the other with the H_2O molecule close to the Ti site. The two starting configurations are represented in Figure 1.

The reaction coordinate Q adopted in this study is the $\text{O}(\text{L})$ –Ti distance, where $\text{O}(\text{L})$ is a H_2O_2 oxygen atom or the H_2O oxygen in the case of water. In the case of H_2O_2 , only one of the two oxygen atoms was constrained at a fixed distance from Ti, whereas the second oxygen atom was completely free.

In each sampling, Q was held fixed and a Car–Parrinello simulation was performed until the force $f(Q)$ necessary to fulfill the $\text{O}(\text{L})$ –Ti constrained distance converged to a stable value $\langle f(Q) \rangle$. Then, a new Q value was chosen, and a further simulation performed with the same criterion. We performed nine constrained simulations in the case of H_2O_2 insertion, whereas seven constrained simulations were sufficient for describing the insertion path of water.

By numerically integrating $-\langle f(Q) \rangle$ along the path for each blue moon sampling, we calculated the free energy profile for the processes.²⁸

They are graphically represented in Figure 2. From inspection of the free energy profiles two main points can be considered: both processes are activated and for both cases the “products”, i.e., the TiLO_4 pentacoordinated center, are more stable than the initial (reagents) state. The relevant geometrical data averaged from the configurations in correspondence of the two

TABLE 1: Averaged O–Ti–O Angles (deg) and Ti–O Distances (Å) for the Free Energy Minima of the Ti(H₂O₂)O₄ and Ti(H₂O)O₄ Complex in Offretite^a

O–Ti–O angles	Ti(H ₂ O ₂)-OFF	Ti(H ₂ O)-OFF
O1–Ti–O2	99.3	95.5
O1–Ti–O3	132.7	136.9
O1–Ti–O4	107.9	107.7
O2–Ti–O3	98.1	95.8
O2–Ti–O4	100.9	99.6
O3–Ti–O4	111.0	110.9
Ti–O distances	Ti(H ₂ O ₂)-OFF	Ti(H ₂ O)-OFF
Ti–O1	1.845	1.812
Ti–O2	1.861	1.856
Ti–O3	1.846	1.877
Ti–O4	1.803	1.856

^a Angles and distances refer to framework oxygen atoms. Atoms labeling as in ref 27.

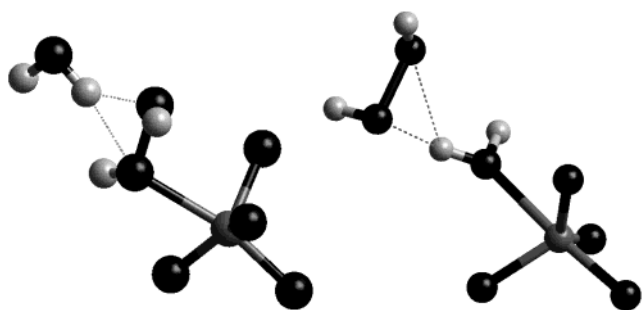


Figure 3. Ball-and-stick representation of a configuration taken from the free energy minimum in the process of insertion of a ligand L at a Ti center in Ti–OFF. In the left panel the Ti(H₂O₂)O₄ center is shown. In the right panel the Ti(H₂O)O₄ center is shown. Only Ti and its four closest oxygen atoms of the full framework are shown. Ti is represented as gray sphere, O as black sphere, hydrogen as light gray sphere. Hydrogen bonds are represented by dotted lines.

free energy minima are reported in Table 1. In both cases the Ti center assumes a distorted trigonal bipyramidal geometry, four vertices are formed by framework oxygen atoms, and the fifth vertex is occupied by the oxygen atom of the ligand. In the equilibrium configuration without ligands,²⁷ Ti assumes a tetrahedral geometry with four framework oxygen atoms at an average distance of 1.821 Å and O–Ti–O angles of 109.4°.

The Ti–O(L) distance resulted 2.24 Å for the water insertion and 2.42 Å for the hydrogen peroxide insertion. Such results are in line with both experimental data on ligands adsorption at Ti site¹⁴ in TS1 and theoretical data from computer simulations.^{26,27}

Inspecting the configurations along the various trajectories in the blue moon sampling yielded an interesting point in both simulations: close to the maximum of the respective free energy profiles, a solvent molecule starts to interact via a hydrogen bond with the ligand molecule and such a hydrogen bond is conserved for both simulations. In ref 27 it was shown that a water molecule should be activated by a hydrogen bond with a second H₂O molecule to form a stable Ti(H₂O)O₄ center in a zeolite. Such a finding is confirmed also by the present blue moon simulations. In the case of H₂O linked to Ti, a H₂O₂ molecule acts as a proton acceptor in a H₂O–H₂O₂ dimer, whereas for the insertion of H₂O₂, a H₂O molecule acts as a proton donor in a H₂O–H₂O₂ dimer. Pictures of the adducts in the free energy minima are represented in Figure 3.

In particular, the Ti(H₂O)O₄ average geometry found in the blue moon sampling is very similar to the one found in standard equilibrium molecular dynamics simulations in hydrated Ti–OFF reported in ref 27.

As far as the energetic of the processes is concerned, we found a free energy stabilization of 2.51 kJ mol^{−1} for water insertion and 1.25 kJ mol^{−1} for hydrogen peroxide insertion. Moreover, we have attempted to force hexacoordination by inserting a second ligand into a pentacoordinated TiLO₄ complex; however, our results indicate that hexacoordinated Ti in Ti–OFF is not stable and they will not be discussed in detail.

For the sake of completeness, we recall that such free energy is relative to the formation of the pentacoordinated Ti complex with respect to the ligand already inside the zeolite channel; therefore the contribution due to the adsorption from the vacuum of the ligand into the zeolite is not accounted for in our calculations. However, when the ligands, H₂O and H₂O₂, are both inside the zeolite, the insertion of H₂O at the Ti center should be energetically favored, and such a finding is in line with the idea that the stronger the basic character of a ligand L, the higher the stability of the Ti(L)O₄ complex.²⁶ However, a key point emerges from the free energy profiles of the two insertion paths, namely, the height of the free energy barrier is higher for H₂O (6.36 kJ mol^{−1}) with respect to that of H₂O₂ (3.64 kJ mol^{−1}). Such a finding indicates that kinetically the hydrogen peroxide insertion should be favored with respect to water insertion. An estimation of the rate *k* (turnover) of the two processes can be obtained by the formula

$$k = (k_B T/h) \exp[-F^\ddagger/k_B T]$$

where *k_B* is the Boltzmann constant, *h* is the Planck constant, and *F[‡]* is the free energy barrier. From such an estimation, it results that both processes are quite fast, of the order of the picosecond; however, the insertion of H₂O₂ is faster (*k* = 1.4 × 10¹² s^{−1}) than the equivalent process for a water molecule (*k* = 0.5 × 10¹² s^{−1}). In other words, though thermodynamics should favor the insertion of water at the Ti center, which could dump the catalytic power of Ti zeolites, kinetics favors the insertion of H₂O₂. This fact may explain why strongly alkaline solutions (i.e., high concentration of OH[−]) inhibit the catalysis, and why a solvent with a lower basic character than water (e.g., methanol) is a good solvent for catalysis.² The structure of the weakly bound Ti(H₂O₂)O₄ complex with a Ti–O(L) equilibrium distance of about 2.42 Å, probably does not correspond to the one of the yellow labile complex.²⁴ Therefore such a nonreactive adsorption of hydrogen peroxide should be considered as the first step toward the formation of the chemically adsorbed yellow complex.

Summary

The formation of complexes with water and hydrogen peroxide at the Ti center of a zeolite has been studied by a combined Car–Parrinello²⁹ statistical perturbation theory²⁸ approach. It is shown that the complex formed by H₂O is thermodynamically more stable, whereas the complex formed by H₂O₂ is kinetically favored.

In this study we have focused our attention only on the formation of a Ti(L)O₄ center without pushing our analysis to the study of the “yellow labile complex”; namely, we have restricted the analysis to the physisorption of H₂O or H₂O₂. What we have been investigating is the competitive attack of the two different ligands to a tetrahedral Ti center in a zeolite structure at room temperature. Actually, to the best of our knowledge such a “physisorbed H₂O₂ complex” has not been experimentally detected; however, a similar weakly bound H₂O₂–TiO₄ complex has been reported in the literature as result of a cluster modeling of the active site in the epoxidation reaction.¹⁸

However, we are now in a position to undertake a study of the reactive path toward the search of such a H₂O₂–zeolite labile complex by starting from a free energy minimum, and moreover, such a structure, even if thermodynamically less stable than the corresponding H₂O adduct, could have a relevant concentration inside the zeolitic channels because of its favorable kinetics.

References and Notes

- (1) Tamarasso, M.; Perego, B.; Notari, B. U.S. Patent 4,410,501, 1983.
- (2) Clerici, M.; Ingallina, P. *J. Catal.* **1993**, *140*, 71–83.
- (3) Notari, B. *Catal. Today* **1993**, *18*, 163–172.
- (4) Vayssilov, G. N. *Catal. Rev. Sci. Eng.* **1997**, *39*, 209–251.
- (5) Lane, B. S.; Burgess, K. *Chem. Rev.* **2003**, *103*, 2457–2473.
- (6) Sinclair, P. E.; Sankar, G.; Catlow, C. R. A.; Thomas, J. M.; Maschmeyer, T. *J. Phys. Chem. B* **1997**, *101*, 4232–4237.
- (7) Lamberti, C.; Bordiga, S.; Arduino, D.; Zecchina, A.; Geobaldo, F.; Spanó, G.; Genoni, F.; Petrini, G.; Carati, A.; Villain, F.; Vlaic, G. *J. Phys. Chem. B* **1998**, *102*, 6382–6390.
- (8) Blasco, T.; Cambor, M. A.; Corma, A.; Pérez-Pariente, J. *J. Am. Chem. Soc.* **1993**, *115*, 11806–11813.
- (9) Lamberti, C.; Bordiga, S.; Zecchina, A.; Crati, A.; Fitch, A. N.; Artioli, G.; Petrini, G.; Salvalaggio, M.; Marra, G. L. *J. Catal.* **1999**, *183*, 222–231.
- (10) Zecchina, A.; Bordiga, S.; Lamberti, C.; Ricchiardi, G.; Lamberti, C.; Ricchiardi, G.; Scarano, D.; Petrini, G.; Leonfanti, G.; Mantegazza, M. *Catal. Today* **1996**, *32*, 97–106.
- (11) Damin, A.; Bonino, F.; Ricchiardi, G.; Bordiga, S.; Zecchina, A.; Lamberti, C. *J. Phys. Chem. B* **2002**, *106*, 7524–7526.
- (12) Bordiga, S.; Damin, A.; Bonino, F.; Zecchina, A.; Spanó, G.; Rivetti, F.; Bolis, V.; Prestipino, C.; Lamberti, C. *J. Phys. Chem. B* **2002**, *106*, 9892–9905.
- (13) Bolis, V.; Bordiga, S.; Lamberti, C.; Zecchina, A.; Crati, A.; Rivetti, F.; Spanó, G.; Petrini, G. *Langmuir* **1999**, *15*, 5753–5764.
- (14) Bordiga, S.; Coluccia, S.; Lamberti, C.; Marchese, L.; Zecchina, A.; Boscherini, F.; Buffa, F.; Genoni, F.; Leonfanti, G.; Petrini, G.; Vlaic, G. *J. Phys. Chem.* **1994**, *98*, 4125–4132.
- (15) Ricchiardi, G.; Damin, A.; Bordiga, S.; Lamberti, C.; Spanó, G.; Rivetti, F.; Zecchina, A. *J. Am. Chem. Soc.* **2001**, *123*, 11409–11419.
- (16) Bellussi, G.; Carati, A.; Clerici, M. G.; Maddinelli, G.; Millini, R. *J. Catal.* **1992**, *133*, 220–230.
- (17) Tozzola, G.; Mantegazza, M. A.; Ranghino, G.; Petrini, G.; Bordiga, S.; Ricchiardi, G.; Lamberti, C.; Zulian, R.; Zecchina, A. *J. Catal.* **1998**, *179*, 64–71.
- (18) Vayssilov, G. N.; van Santen, R. A. *J. Catal.* **1998**, *175*, 170–174.
- (19) Munakata, H.; Oumi, Y.; Miyamoto, A. *J. Phys. Chem. B* **2001**, *105*, 3493.
- (20) Neurock, M.; Manzer, L. E. *Chem. Commun.* **1996**, 1133.
- (21) Karlsen, E.; Shoffel, K. *Catal. Today* **1996**, *32*, 107.
- (22) Sever, R. R.; Root, T. W. *J. Phys. Chem. B* **2003**, *107*, 4080.
- (23) Sever, R. R.; Root, T. W. *J. Phys. Chem. B* **2003**, *107*, 4090.
- (24) Bordiga, S.; Damin, A.; Bonino, F.; Ricchiardi, G.; Lamberti, C.; Zecchina, A. *Angew. Chem., Int. Ed.* **2002**, *41*, 4734–4735.
- (25) Damin, A.; Bordiga, S.; Zecchina, A.; Lamberti, C. *J. Chem. Phys.* **2002**, *117*, 226.
- (26) Damin, A.; Bordiga, S.; Zecchina, A.; Doll, K.; Lamberti, C. *J. Chem. Phys.* **2003**, *118*, 10183.
- (27) Fois, E.; Gamba, A.; Spanó, E. *J. Phys. Chem. B* **2004**, *108*, 154–159.
- (28) Carter, E. A.; Ciccotti, G.; Hynes, J. T.; Kapral, R. *Chem. Phys. Lett.* **1989**, *165*, 472.
- (29) Car, R.; Parrinello, M. *Phys. Rev. Lett.* **1985**, *55*, 2471–2474.
- (30) Sprik, M.; Ciccotti, G. *J. Chem. Phys.* **1998**, *109*, 7737.
- (31) Curioni, A.; Sprik, M.; Andreoni, W.; Shiffer, H.; Hutter, J.; Parrinello, M. *J. Am. Chem. Soc.* **1997**, *119*, 7218.
- (32) Fois, E.; Gamba, A.; Tabacchi, G. *Chem. Phys. Lett.* **2000**, *329*, 1.
- (33) Tilocca, A.; Selloni, A. *J. Chem. Phys.* **2003**, *119*, 7445.
- (34) Mortier, W. J.; Pluth, J. J.; Smith, J. V. *Z. Kristallogr.* **1976**, *143*, 319–332.
- (35) Kwak, J. H.; Cho, S. J.; Ryoo, R. *Catal. Lett.* **1996**, *37*, 217–221.
- (36) Campana, L.; Selloni, A.; Weber, J.; Goursot, A. *J. Phys. Chem.* **1997**, *99*, 16351.
- (37) Becke, A. D. *Phys. Rev. A* **1988**, *38*, 3098.
- (38) Perdew, J. P. *Phys. Rev. B* **1986**, *33*, 8822.
- (39) Kleinman, L.; Bylander, D. *Phys. Rev. Lett.* **1982**, *48*, 1425.
- (40) Troullier, N.; Martins, J. L. *Solid State Commun.*, **1990**, *74*, 613–616.
- (41) Kohn, W.; Sham, L. J. *Phys. Rev. A* **1965**, *140*, 1133–1138.
- (42) CPMD 3.3, written by J. Hutter et al., MPI für Festkörperforschung and IBM Research Laboratory.
- (43) Nose, S. *J. Chem. Phys.* **1984**, *81*, 511.